Effect of Aluminum Substitution in C-S-H on Viscoelastic Properties: Stress Relaxation Nanoindentation

William A. Hunnicutt[1], Paramita Mondal[2] and Leslie J. Struble[3]

Abstract

Creep in concrete is thought to originate in the primary hydration product of Portland cement, the semi-amorphous calcium silicate hydrate (C-S-H). The molecular structure and chemical composition of C-S-H are variable and it is expected that this variability affects mechanical properties, specifically viscoelasticity. In this study the correlation between molecular structure and viscoelastic properties in C-S-H is explored by examining the role of aluminum substitution for silicon. Solid-state nuclear magnetic resonance spectroscopy is used to probe molecular structure and stress relaxation nanoindentation is used to measure viscoelastic properties of synthesized C-S-H with and without aluminum substitution. Results show that the addition of aluminum increases the aluminosilicate mean chain length and the crosslinking, and that the substitution of aluminum for silicon in C-S-H produces less viscous behavior. It is known that supplementary cementitious materials can provide the aluminum required for this substitution in concrete, so the knowledge gained will provide a practical way to reduce viscoelastic deformation in concrete structures.

1. First Author is a Ph.D student at the University of Illinois at Urbana-Champaign, Urbana, IL 61801 (email:hunnctt2@illinois.edu).
2. Second Coauthor is an Assistant Professor at the University of Illinois at Urbana-Champaign, Urbana, IL 61801 (email:pmondal@illinois.edu).
3. Third Coauthor is a Professor Emeritus at the University of Illinois at Urbana-Champaign, Urbana, IL 61801 (email:lstruble@illinois.edu).

I. INTRODUCTION

Concrete infrastructure is a critical component of a society and tremendous care must be taken to properly design and maintain the concrete. Not only is the economic cost of reconstruction high, so is the environmental cost. These high costs mean that it is critical to design the concrete for a long service life. One of the material properties of concrete often ignored when designing a concrete mix is its viscoelastic behavior.

Pre-stressed concrete bridge members provide an example of how viscoelastic behavior can lead to a reduction in load carrying capacity. Steel tendons are placed and tensioned while the concrete is fresh, and tension is released after several days of curing, placing concrete in the area of the tendons under compression. The viscoelastic behavior allows the concrete to "flow" when under stress for a long period of time, reducing the compressive stress. The resulting loss of load carrying capacity can be mitigated by modifying the concrete such that the viscous response is reduced.

Our goal in this study is to explore whether the viscous response of the calcium silicate hydrate (C-S-H), the primary hydration product of Portland cement, is correlated with it's the molecular structure. More specifically, we are using aluminum substitution for silicon in C-S-H to vary the molecular structure and, perhaps, the viscoelastic properties.

II. BACKGROUND

The structure of C-S-H is broadly understood to be calcium oxide sheet sandwiched by short and discrete silicate chains [1]-[3]. The chains are comprised of repeating units of tetrahedral silica in a "dreierketten" arrangement; three tetrahedra, one bridging and two pairing. The pairing tetrahedra share two oxygen atoms with the calcium oxide sheet while the bridging tetrahedra share only one oxygen atom [4]. Aluminum readily enters the molecular structure of C-S-H, typically by replacing a tetrahedral silicon in the bridging position. This substitution promotes the growth of the aluminosilicate chain and crosslinking [5]-[7]. Presented in Fig. 1 is an idealized molecular structure of C-A-S-H showing tetrahedra at the end of chains (Q^1), tetrahedra in the middle of chains (Q^2), and tetrahedral crosslinking chains through one alumina tetrahedron ($Q^3(1Al)$).

The molecular structure of the C-S-H phase is thought to play a major role in the viscoelastic nature of hardened cement paste and concrete [8]-[12]. Aging increases MCL [13] and reduces the viscous response [14]. Curing at higher temperatures increases the MCL [13] and reduces the viscous response of hydrated alite samples [12]. Alizadeh et al. [15], using dynamic mechanical analysis, showed that an increase in MCL corresponds to an increase in elastic modulus and a decrease in loss factor (loss modulus/storage modulus).

In order to study the mechanical properties of C-S-H the phase must be synthesized. Hydration is not preferred because other products form alongside the C-S-H, such as calcium hydroxide, and because it does not allow control of the Al-content. When using synthesized C-S-H, it is convenient to mechanically test very small samples, on the order of millimeters, and nanoindentation measurements are well suited because they allow a large number of measurements on a small sample. Also, because the interaction volume is small, nanoindentation is more sensitive to small changes in mechanical behavior due to the modification of the molecular structure.

The often-used Oliver-Pharr method of determining the elastic modulus uses the initial section of the unloading curve of a load-controlled nanoindentation experiment to determine the modulus,

$$\{1\} S = \frac{dP}{dh} = \frac{2}{\sqrt{\pi}} E_r \sqrt{A},$$

where $S=dP/dh$ is the measured stiffness of the initial unloading curve on the load-displacement plot, E_r is the reduced modulus, and A is the projected contact area. The reduced modulus is defined as

$$\{2\} \frac{1}{E_r} = \frac{1-\nu^2}{E} + \frac{1-\nu_i^2}{E_i},$$

where E and ν are the Young's modulus and Poisson's ratio of the specimen, and E_i and ν_i are the same parameters for the indenter [16].

The Oliver-Pharr method works well for elastic properties, but determining viscoelastic properties requires a different method, broadly classified as dynamic or quasi-static with long hold period. Dynamic methods have the advantages of a shorter experimentation time and direct measurement of the phase lag between stress and strain;

Fig. 1. Idealized molecular structure of C-A-S-H.

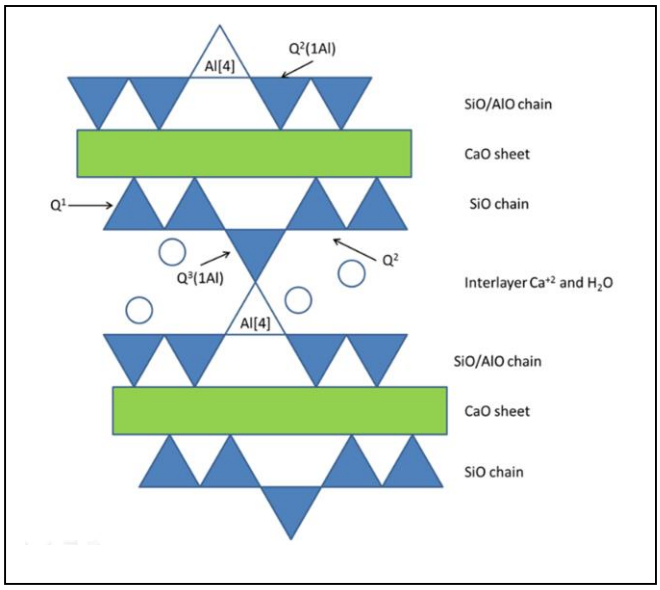

however, for materials with low loss (such as hydrated cement paste) subresonant dynamic methods typically available in nanoindentation do not work particularly well [17]. The two most common quasi-static methods are creep (constant load) and stress relaxation (constant displacement). Others have used nanoindentation creep experiments to characterize the viscoelastic behavior of hydrated cement paste with some success [18] [19]. No use of stress relaxation nanoindentation on hydrated cement has been found, but it has seen limited use in other materials systems [20]. We have conducted nanoindentation creep experiments on C-(A)-S-H with unsatisfactory results--large drift during indentation, mediocre goodness-of-fit, and wide confidence intervals. The unsuccessful creep measurements led to our use in this paper of stress relaxation to characterize the viscoelastic behavior of C-(A)-S-H.

III. METHODS

A. Synthesis

C-S-H and C-A-S-H have been synthesized using stoichiometric proportions of CaO (freshly calcined $CaCO_3$), fumed silica (SiO_2), and aluminum nitrate nonahydrate ($AlN_3O_9{\cdot}9H_2O$) to yield C-S-H with Ca/Si=1.0 and C-A-S-H with Ca/Si=1.0 and Al/Si=0.2. The reagents were mixed in excess degassed, deionized water in a screw-top high-density polyethylene bottle in a nitrogen-filled glovebox, continuously agitated for two weeks, filtered in a nitrogen-filled glovebox, and dried in a vacuum oven at 40°C for 24 hours. The dried powder was ground with a mortar and pestle in a nitrogen environment to pass a 75-µm sieve and equilibrated at 11% relative humidity (by storing in a vacuum desiccator over a saturated solution of LiCl in water).

B. Chemical Characterization

The C-S-H and C-A-S-H were chemically characterized using x-ray diffraction (XRD), thermogravimetric analysis (TGA), and ^{29}Si solid-state nuclear magnetic resonance spectroscopy (NMR). The XRD analysis was performed to identify any crystalline phases due to carbonation. A powder diffractometer with Cu-Kα radiation in the theta/theta configuration and operated at 40 kV and 30 mA was used for this purpose, and specimens were scanned from 10° to 60° 2θ at a rate of 1°/min with a step size of 0.02° 2θ. The diffraction patterns were analyzed using XRD analysis software in which peaks were matched to the patterns in the standard powder diffraction file. The TGA was performed to quantify the amount of $CaCO_3$ present as a result of carbonation. Minimization of $CaCO_3$ in the samples is important since it is an inhomogeneity in the C-(A)-S-H that might affect the mechanical response, possibly confounding results. Alumina crucibles were used and the specimen weight was approximately 10 mg. The specimen was heated at 10°C/min from room temperature to 105°C, held at 105°C for 5 minutes to remove loosely bound water, then heated to 1000°C also at 10°C/min. The entire experiment took place in nitrogen flowing at 60 mL/min. The ^{29}Si NMR was performed to characterize the local atomic structure of ^{29}Si nuclei. The spectrometer (300 MHz, 7.05 T) was operated at 59.6 MHz using a 4-mm probe spinning at 10 kHz, direct polarization, a π/2 flip angle with ^{1}H decoupling, a recycle delay of 60 s, and an acquisition time of 20.48 ms. In total, 1536 scans were collected and summed for each specimen. Chemical shifts were measured relative to tetramethylsilane. Deconvolution of the spectra was conducted using a commercial software package.

C. Mechanical Characterization

The dried C-S-H and C-A-S-H powders were compacted using a 25.4-mm diameter die and a hydraulic load frame. For each specimen, 2.0 g were compacted at 250 kN. The piston of the compaction die had been finely polished using a 0.04-µm colloidal silica suspension and seen to imprint a smooth and flat surface on the compacted powder so no polishing of the compacted pellets was required. The compaction method was shown previously to provide mechanical properties that agree well with those of a hydrated cement paste [9]. A ^{29}Si NMR analysis of uncompacted C-S-H powder and a powdered C-S-H compact showed no significant changes in molecular structure during compaction.

Quasi-static displacement controlled nanoindentation experiments were performed on compacts of C-S-H and C-A-S-H using a diamond Berkovich tip. The indentations followed a 10x20 grid with 10 µm between indents. For the stress relaxation experiment a trapezoidal load function in displacement control was used, the compacts were indented to a depth of 175 nm over a period of 1 second, held at this displacement for 60 seconds, and unloaded over 1 second (Fig. 2). The fast loading and unloading rates were used to approximate a Heaviside function. Force was measured as a function of time. The load-displacement curves for each indent were examined to identify any erroneous indents and

Fig. 2. Stress relaxation load function.

these indents were not considered during analysis. For the C-S-H 32 indents were removed for the C-A-S-H 4 indents were removed. The force and time data during the hold period were fitted to a two-term exponential function and the force was normalized for each indent in order to compare the C-S-H and C-A-S-H. Statistical analysis was performed and 99.8% confidence intervals were developed.

IV. RESULTS AND DISCUSSION

A. Chemical Characterization

XRD results in Fig. 3 indicate that C-S-H and C-A-S-H were successfully synthesized. Several small calcite peaks are present in the C-A-S-H sample, but there is no apparent carbonation of the C-S-H. The peaks associated with C-S-H are better defined for the C-S-H sample than the C-A-S-H sample.

The TGA results allow for a quantitative determination of carbonation. The region of mass loss associated with the thermal decomposition of $CaCO_3$ is taken as 550°-1000° C. The mass loss in this range is 3.5% for C-S-H and 4.3% for C-A-S-H. The TGA data are consistent with the XRD data, in that the C-A-S-H has more mass loss above 550° C and better defined calcite peaks. In both C-S-H and C-A-S-H the amount of carbonation is small and assumed to have no effects on mechanical properties.

The ^{29}Si NMR results are presented in Fig. 4 and Table 1. The peak assignments are based on those by Sun et al. and others [5] [6] [21] [22]. The deconvolution results are consistent with a dreierketten structure with aluminum only substituting silicon in the bridging position, in that the ratio of bridging tetrahedra to pairing tetrahedra is approximately ½ and the ratio $Q^2(1Al)/Q^3(1Al)\approx 2$. Crosslinking ($Q^3$) is present in the C-A-S-H but not in the C-S-H. The MCL can be calculated according to [7]

$$\{3\}MCL = \frac{Q^1+Q^2{}_B+Q^2{}_P+\frac{3}{2}Q^2(1Al)+Q^3+Q^3(1Al)}{\frac{1}{2}Q^1}.$$

The MCL of the C-S-H is 7.5 and the MCL of the C-A-S-H is 28.3. The addition of aluminum to C-S-H produces changes in molecular structure consistent with the literature: longer MCL and presence of crosslinking (evidenced by Q^3).

Fig. 3. XRD pattern of C-S-H (top) and C-A-S-H (bottom). CSH=C-S-H peak, C=calcite peak.

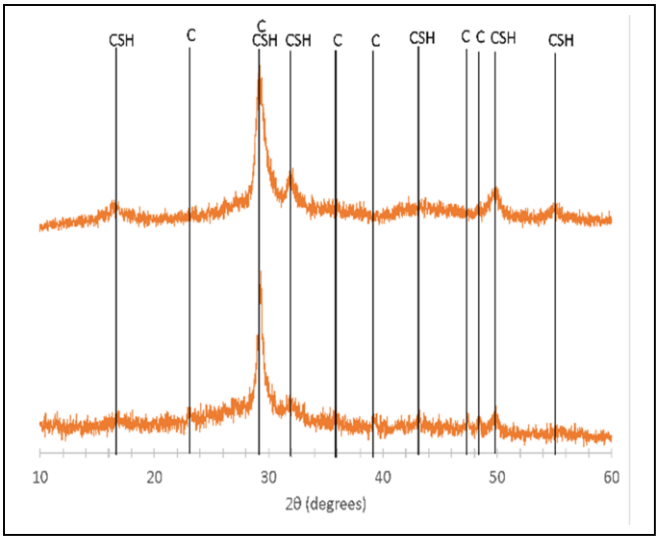

C. Mechanical Characterization

A histogram of the indentation load at the beginning of the hold period during the stress relaxation experiment is presented in Fig. 5 and at the end of the hold period in Fig. 6.

Fig. 4. ^{29}Si NMR for C-S-H (top) and C-A-S-H (bottom). Original spectrum (red), deconvoluted peaks (blue), and summation of deconvoluted peaks (black).

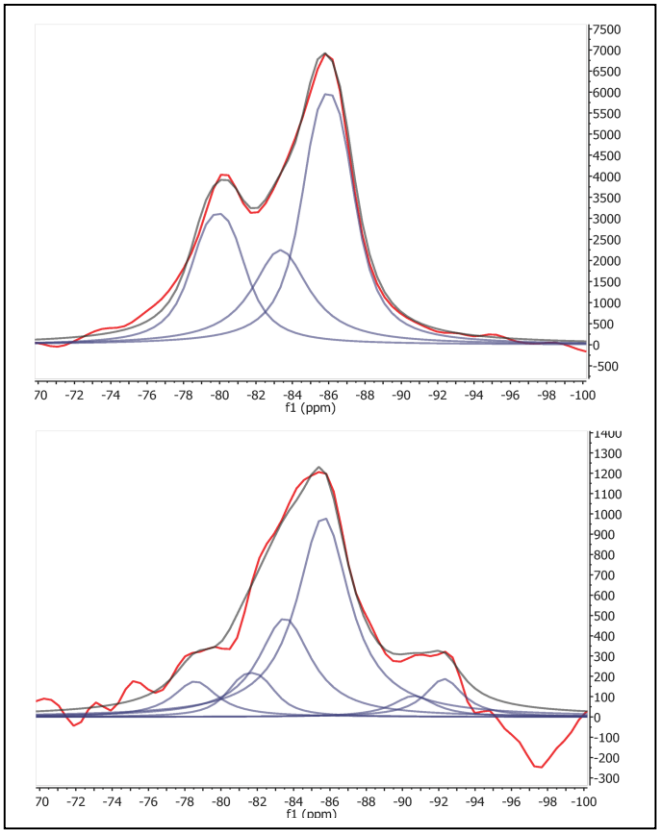

Table 1. ^{29}Si deconvolution results for C-S-H and C-A-S-H.

Sample	Local environment					
	Q^1	$Q^2(1Al)$	$Q^2{}_B$	$Q^2{}_P$	$Q^3(1Al)$	Q^3
C-S-H	27%	-	24%	49%	-	-
C-A-S-H	7%	8%	24%	50%	4%	7%

The maximum load at a displacement of 175 nm is greater for the C-S-H than the C-A-S-H, indicating that C-S-H has a higher elastic modulus. The relationship between MCL and elastic modulus observed here is not consistent with the work conducted by Alizadeh et al. [15], where a higher MCL is associated with a higher elastic modulus. The most likely reason for this difference is that the compaction of C-S-H and C-A-S-H at 250 kN produced compacts of different porosities due to physical differences between the C-S-H and C-A-S-H.

The viscoelastic properties of the C-S-H and C-A-S-H are first examined by the difference in load at the beginning and end of the 60 s hold period. In addition to the histograms in Fig. 5 and 6, a one-tailed two-sample t-test was performed. There was a significant difference in the change in load over the hold period for the C-S-H (mean=267.3 μN, standard deviation=84.4) and C-A-S-H (mean=172.3 μN, standard deviation=36.1) with p-value=4.1×10^{-31}. In an attempt to take into account the difference in elastic properties between the C-S-H and C-A-S-H the measured force was normalized by the maximum load at the beginning of the constant displacement hold period. The resulting normalized force curves as a function of time are presented in Fig. 7. The mean coefficient of determination for the fitting procedure is greater than 0.97 for each sample, indicating that the data are well fitted by a two-term exponential function. The dotted lines correspond to 99.8% confidence intervals. The tight distribution of normalized force data indicates that the viscoelastic properties are not greatly affected by the inhomogeneities or surface roughness.

The C-A-S-H has a higher normalized force than C-S-H at every time in this experiment, i.e., the stress relaxed more quickly in the C-S-H than the C-A-S-H. A higher normalized force curve indicates that the C-A-S-H, with its higher MCL and greater crosslinking, is behaving less viscously than the C-S-H. These observations are consistent with viscoelastic results provided by others [12]-[15]. It interesting and worth noting that the C-S-H exhibits more load relaxation than the C-A-S-H even though the elastic modulus of the C-S-H is higher than the C-A-S-H. The implications of this observation deserve additional attention.

Fig. 5. Histogram of load at beginning of hold period during stress relaxation of C-S-H and C-A-S-H.

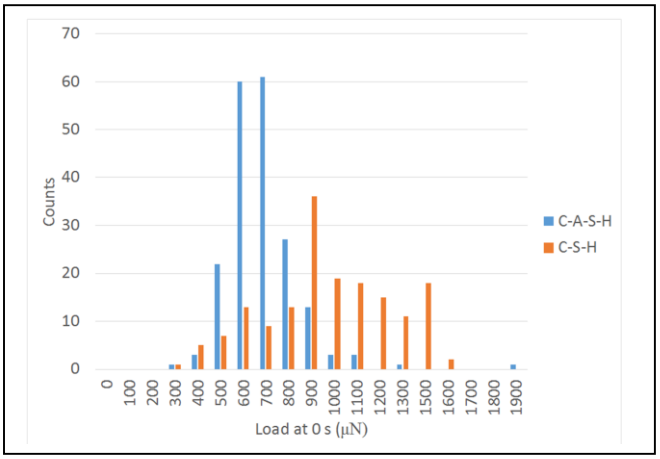

Fig. 6. Histogram of load at end of hold period during stress relaxation of C-S-H and C-A-S-H.

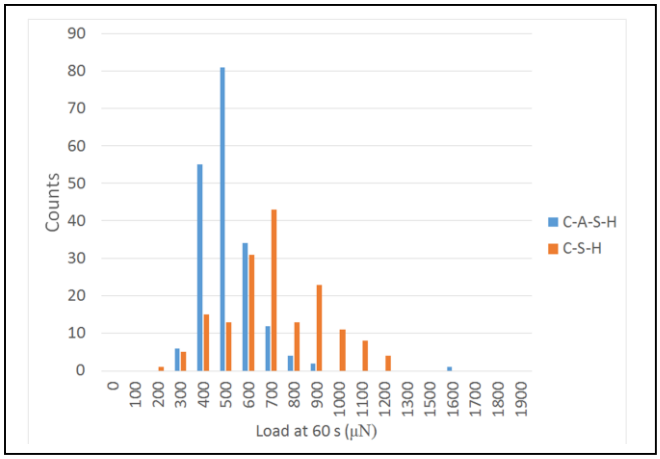

The viscoelastic response of the semi-amorphous C-(A)-S-H appears to be based on layers or particles continuously moving relative to each other under sustained stress. Several more detailed viscoelastic mechanisms have been presented that include effects of particle shape, but they are still predicated on relative movement of particles [18] [23] [24]. The relationship between molecular structure of C-(A)-S-H and the viscoelastic mechanism is best thought of in terms of particle size. When C-(A)-S-H has a longer MCL and exhibits crosslinking, it has fewer particles for a given amount of material. This reduction in particle number reduces the probability of relative particle movement and thus reduces the viscous response of the material.

Fig. 7. Normalized stress relaxation nanoindentation of C-S-H and C-A-S-H showing 99.8% confidence intervals.

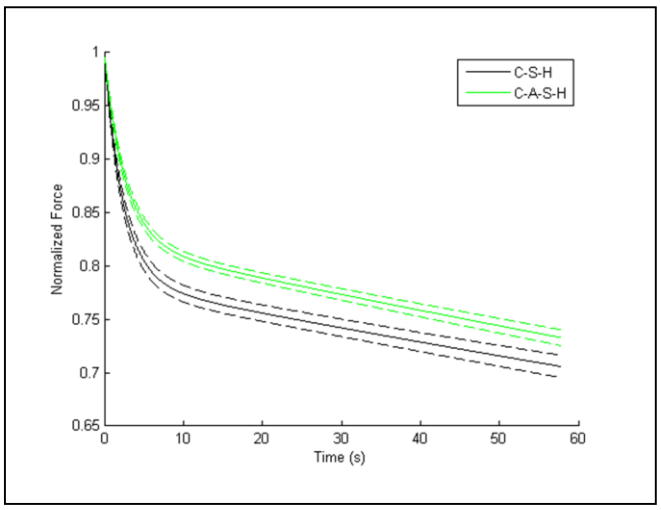

V. CONCLUSIONS

Synthesis and characterization of C-S-H and C-A-S-H were performed. Limited carbonation was observed and its effect on viscoelastic behavior is thought to be minimal. The addition of aluminum to C-S-H causes an increase in the mean length of the aluminosilicate chain and an increase in crosslinking between layers. The increased MCL and crosslinking of C-A-S-H are considered to be responsible for the lower viscous response compared to C-S-H. The difference in elastic modulus between the C-S-H and C-A-S-H does not appear to significantly affect the stress relaxation behavior.

REFERENCES

[1] X. Cong and R. Kirkpatrick, "29Si MAS NMR study of the structure of calcium silicate hydrate," *Advanced Cement Based Materials,* vol. 3, pp. 144-156, 1996.

[2] H. Taylor, "Proposed structure for calcium silicate hydrate gel," *Journal of the American Ceramics Society,* vol. 69, pp. 464-467, 1986.

[3] I. Richardson, "The nature of C-S-H in hardened cements," *Cement and Concrete Research,* vol. 29, pp. 1131-1147, 1999.

[4] I. Richardson, "The calcium silicate hydrates," *Cement and Concrete Research,* vol. 38, pp. 137-158, 2008.

[5] G. Sun, J. F. Young and R. J. Kirkpatrick, "The role of Al in C-S-H: NMR, XRD, and compositional results for precipitated samples," *Cement and Concrete Research,* vol. 36, pp. 18-29, 2006.

[6] P. Faucon, A. Delagrave, J. Petit, C. Richet, J. Marchand and H. Zanni, "Aluminum incorporation in calcium silicate hydrates (C-S-H) depending on their Ca/Si ratio," *Journal of Physical Chemistry B,* vol. 103, no. 37, pp. 7796-7802, 1999.

[7] W. Hunnicutt, Characterization of calcium-silicate-hydrate and calcium-alumino-silicate-hydrate, Urbana: University of Illinois at Urbana-Champaign, 2013.

[8] B. Tamtsia and J. Beaudoin, "Basic creep of hardened cement paste: A re-examination of the role of water," *Cement and Concrete Research,* vol. 30, pp. 1465-1475, 2000.

[9] R. Feldman, "Factors affecting the Young's modulus - porosity relation of hydrated Portland cement compacts," *Cement and Concrete Research,* vol. 2, pp. 375-386, 1972.

[10] A. Bentur, N. Milestone and J. Young, "Creep and drying of calcium silicate pastes II. Induced microstructural and chemical changes," *Cement and Concrete Research,* vol. 8, pp. 721-732, 1978.

[11] A. Bentur, N. Milestone and J. Young, "Creep and drying of calcium silicate pastes III. A hypothesis of irreversible strains," *Cement and Concrete Research,* vol. 9, pp. 83-96, 1979.

[12] A. Bentur, N. Milestone and J. Young, "Creep and drying of calcium silicate pastes IV. Effects of accelerated curing," *Cement and Concrete Research,* vol. 9, pp. 161-170, 1979.

[13] J. Hirljac, Z. Wu and J. Young, "Silicate polymerization during the hydration of alite," *Cement and Concrete Research,* vol. 13, pp. 877-886, 1983.

[14] G. Verbeck and R. Helmuth, "Structures and physical properties of cement paste," in *Proceedings of the 5th International Symposium on the Chemistry of Cement*, Tokyo, 1969.

[15] R. Alizadeh, J. Beaudoin and L. Raki, "Mechanical properties of calcium silicate hydrates," *Materials and Structures,* vol. 44, no. 1, pp. 13-28, 2011.

[16] W. Oliver and G. Pharr, "An improved technique for determining hardness and elastic modulus using load and displacement sensing indentation experiments," *J. Mater. Res.,* vol. 7, no. 6, pp. 1564-1583, 1992.

[17] R. Lakes, Viscoelastic Materials, Cambridge: Cambridge University Press, 2009.

[18] M. Vandamme and F.-J. Ulm, "Nanoindentation investigation of creep properties of calcium silicate hydrates," *Cement and Concrete Research,* vol. 52, pp. 38-52, 2013.

[19] C. Jones and Z. Grasley, "Short-term creep of cement paste during nanoindentation," *Cement and Concrete Composites,* vol. 34, pp. 468-477, 2012.

[20] J. Kaufman, G. Miller, E. Morgan and C. Klapperich, "Time-dependent mechanical characterization of poly(2-hydroxyethyl methacrylate) hydrogels using nanoindentation and unconfined compression," *J. Mater. Res.,* vol. 23, no. 5, pp. 1472-1481, 2008.

[21] I. Garcia Lodeiro, A. Fernandez-Jimenez, A. Palomo and D. Macphee, "Effect on fresh C-S-H gels of the simultaneous addition of alkali and aluminum," *Cement and Concrete Research,* vol. 40, pp. 27-32, 2010.

[22] H. Manzano, J. Dolado, M. Griebel and J. Hamaekers, "A molecular dynamics study of the aluminosilicate chains structure in Al-rich calcium silicate hydrated (C-S-H) gels," *Physica Status Solidi A,* vol. 205, no. 6, pp. 1324-1329, 2008.

[23] R. Alizadeh, J. Beaudoin and L. Raki, "Viscoelastic nature of calcium silicate hydrate," *Cement and Concrete Composites,* vol. 32, pp. 369-376, 2010.

[24] M. Vandamme and F.-J. Ulm, "The nanogranular origin of creep," *Proceedings of the National Academy of Sciences,* vol. 106, no. 26, pp. 10552-10557, 2009.